JOURNAL OF VIROLOGY, Dec. 1997, p. 9295–9305 Vol. 71, No. 12
0022-538X/97/$04.00+0

Distinct Functions and Requirements for the Cys-His Boxes of the Human Immunodeficiency Virus Type 1 Nucleocapsid Protein during RNA Encapsidation and Replication

MICHAEL D. SCHWARTZ, DICCON FIORE, AND ANTONITO T. PANGANIBAN*

McArdle Laboratory for Cancer Research, University of Wisconsin Medical School, Madison, Wisconsin 53706

Received 13 June 1997/Accepted 22 August 1997

The process of retroviral RNA encapsidation involves interaction between *trans*-acting viral proteins and *cis*-acting RNA elements. The encapsidation signal on human immunodeficiency virus type 1 (HIV-1) RNA is a multipartite structure composed of functional stem-loop structures. The nucleocapsid (NC) domain of the Gag polyprotein precursor contains two copies of a Cys-His box motif that have been demonstrated to be important in RNA encapsidation. To further characterize the role of the Cys-His boxes of the HIV-1 NC protein in RNA encapsidation, the relative efficiency of RNA encapsidation for virus particles that contained mutations within the Cys-His boxes was measured. Mutations that disrupted the first Cys-His box of the NC protein resulted in virus particles that encapsidated genomic RNA less efficiently and subgenomic RNA more efficiently than did wild-type virus. Mutations within the second Cys-His box did not significantly affect RNA encapsidation. In addition, a full complement of wild-type NC protein in virus particles is not required for efficient RNA encapsidation or virus replication. Finally, both Cys-His boxes of the NC protein play additional roles in virus replication.

The core of human immunodeficiency virus type 1 (HIV-1) particles is composed mainly of proteins expressed from the *gag* and *pol* genes. The Gag precursor, $Pr55^{gag}$, and the Gag-Pol precursor, $Pr160^{gag\text{-}pol}$, are initially synthesized as polyproteins (77), and assembly and release of HIV-1 particles occur at the plasma membrane where $Pr55^{gag}$ and $Pr160^{gag\text{-}pol}$ are associated with the plasma membrane by way of N-terminal hydrophobic amino acids (74, 80) and an N-terminal myristic acid residue (11, 28). $Pr55^{gag}$ is the only viral protein required for virus particle formation (24, 30). During assembly or budding of the virus particle, a virally encoded protease proteolytically processes the Gag polyprotein into the matrix (MA, p17), capsid (CA, p24), p2, nucleocapsid (NC, p7), p1, and $p6^{gag}$ proteins (28, 45, 60, 65). Proteolytic processing is not required for efficient HIV-1 particle assembly or release (28, 45, 65) but is required for the production of mature, infectious particles (35, 45, 65).

An essential component of the HIV-1 particle is dimeric, unspliced, genomic-length viral RNA (51). The process by which this RNA becomes associated with the virus particle is termed RNA encapsidation or packaging. RNA encapsidation is highly specific, since greater than 95% of RNA found in particles is viral RNA, although viral RNA makes up only about 1% of the total cytoplasmic mRNA found in cells. Encapsidation also results in the preferential encapsidation of unspliced, genomic-length viral RNA; more than 95% of viral RNA found in virus particles is unspliced, genomic-length RNA, even though subgenomic RNA makes up about half of the viral RNA found in the cytoplasm of virus-producing cells.

Encapsidation requires interaction between *cis*-acting sequences on viral RNA and proteins of the assembling virus particle. *cis*-acting sequences involved in HIV-1 RNA encapsidation are located near the 5′ ends of the viral genome (3, 13, 32, 42, 50, 54, 56, 64, 72). In vitro biochemical probing, computer modeling, and phylogenetic comparisons suggest that the secondary structure at the 5′ end of HIV-1 RNA consists of seven stem-loop structures (4, 14, 31, 69). The importance of some of these stem-loop structures in RNA encapsidation in vivo has been confirmed (46, 56, 57, 78). It is likely that higher-order RNA structure, rather than primary nucleotide sequence, is involved in RNA encapsidation (57, 78). Some of the *cis*-acting sequences that have been implicated in HIV-1 RNA encapsidation are contained on both genomic and subgenomic RNA (3, 6, 7, 13, 14, 42, 50, 54, 56, 68). Because retroviruses contain both intronic and exonic encapsidation signals, it is not yet clear how preferential encapsidation of genomic RNA over subgenomic RNA occurs.

There is strong evidence that the Gag polyprotein precursor is involved in RNA encapsidation. Moreover, virus particles produced in the absence of the *pol* and *env* gene products specifically encapsidate viral RNA (39, 61, 70), suggesting that the Gag protein is sufficient for RNA encapsidation. One domain of $Pr55^{gag}$ that is involved in RNA encapsidation is the nucleocapsid (NC) protein domain, since mutations within NC have been demonstrated to affect RNA encapsidation in vivo (3, 19, 25, 27, 62, 66) and RNA binding in vitro (7, 15, 18, 53, 71). During the initial interaction with viral RNA, the NC protein most likely acts as part of $Pr55^{gag}$, since proteolytic processing is not required for efficient RNA encapsidation (39). The mature HIV-1 NC protein is 55 amino acid residues in length and contains many basic amino acid residues. Mutations that affect some of the basic amino acid residues of HIV-1 NC reduce RNA encapsidation in vivo (19, 66) and RNA binding in vitro (71). The mature NC protein is closely associated with genomic RNA in mature virions (16) and has been demonstrated to have both nonspecific (17, 37, 40, 49, 52, 59) and specific (7, 14, 15, 34, 53) RNA binding activities in

* Corresponding author. Mailing address: McArdle Laboratory for Cancer Research, University of Wisconsin Medical School, 1400 University Ave., Madison, WI 53706. Phone: (608) 263-7820. Fax: (608) 262-2824. E-mail: Panganiban@oncology.wisc.edu.

vitro. Analysis of chimeric Gag proteins has provided some evidence that the NC protein provides at least some specificity for viral RNA during encapsidation in vivo (8, 21, 70, 79).

With the exception of spumaretroviruses, all known retroviruses contain at least one copy of the sequence Cys-X_2-Cys-X_4-His-X_4-Cys, termed a cysteine-histidine (Cys-His) box or motif. Retrovirus Cys-His boxes resemble zinc finger domains found in many nucleic acid binding proteins (5), and the HIV-1 NC protein contains two Cys-His boxes that are capable of binding Zn^{2+} (9). The Cys-His boxes of HIV-1 have been shown to play a critical role in RNA encapsidation, since mutations that alter the cysteine or histidine residues of NC reduce the efficiency of RNA encapsidation (3, 20, 25–27, 33, 79).

Mutational analysis of NC proteins that contain two Cys-His boxes indicates that the boxes are not functionally equivalent (10, 25) and that the first Cys-His box of HIV-1 NC appears to be more important for HIV-1 RNA encapsidation (25). Deletion of the first Cys-His box of HIV-1 NC and mutations that disrupt both Cys-His boxes of HIV-1 NC have been demonstrated to increase the encapsidation efficiency of subgenomic RNA (8, 79).

To further characterize the role of the HIV-1 NC protein in efficient and specific RNA encapsidation, mutant virus particles that contained mutations within the Cys-His boxes were analyzed. Results indicated that mutation of the first two cysteine residues of Cys-His box 1 leads to both a decrease in the efficiency of genomic RNA encapsidation and an increase in the efficiency of subgenomic RNA encapsidation. Analysis of heterogeneous virus particles containing both wild-type (WT) and NC mutant Gag molecules revealed that a full complement of WT Gag molecules is not required for efficient or specific genomic RNA encapsidation or for virus replication.

MATERIALS AND METHODS

Maintenance of cell lines, transfections, and infections. Two hundred ninety-three cells were maintained in Dulbecco's modified Eagle's medium supplemented with 10% fetal bovine serum (HyClone), 0.05 mg of gentamicin (Gibco BRL) per ml, and 10 mM HEPES (Gibco BRL) and incubated at 37°C at 5% CO_2. Twenty-four hours prior to transfection, 293 cells were seeded at a density of 2.5×10^6 cells per 100-mm-diameter cell culture dish. Transfections were carried out by a modified calcium phosphate precipitation method (2). Briefly, 10 μg of plasmid DNA was suspended in 0.5 ml of a solution containing 125 mM $CaCl_2$. An equal volume of 2× BES buffer {50 mM BES [*N*,*N*-bis(2-hydroxyethyl)-2-aminosulfonic acid], 280 mM NaCl, 1.5 mM $Na_2HPO_4 \cdot 2H_2O$ (pH 6.96)} was added, and the DNA was incubated at room temperature for 45 min. This precipitate solution was added to a 100-mm-diameter plate, and the cells were incubated at 37°C and 5% CO_2 for 16 to 20 h. The medium was then removed, fresh medium was added, and the cells were incubated for an additional 48 h.

Infectivity assays were performed as previously described with CD4-long terminal repeat (LTR)/β-galactosidase (β-Gal) (23, 43). Briefly, 293 cells were transfected as described above, except that 15 μg of DNA/plate (7.5 μg of pSV-A-MLV and 7.5 μg of virus expression plasmid) was transfected. DEAE-dextran was added to a final concentration of 80 μg/ml, and 500 μl of media was used to infect 3×10^4 CD4-LTR/β-Gal cells per 24-well cell culture plate. CD4-LTR/β-Gal cells were assayed for β-Gal expression 2 days after infection.

Construction of plasmid DNAs. Standard molecular cloning techniques (55) were used to generate plasmids. pMSMΔEnv2 is a derivative of the infectious proviral clone pNL4-3 (1). The nucleotide designations refer to the DNA sequence of pNL4-3. The construction of pMSMΔEnv2 has been previously described (56), and this plasmid is identical to pMSMBA (also previously described [56]), except that pMSMΔEnv2 retains the naturally occurring *Bsp*EI site at base pair (bp) 9383 in the distal LTR.

pNC1 was created by PCR amplification of pMSMΔEnv2 with the sense primer 1465–1485 (5′-GGC CAG ATG AGA GAA CCA AGG) and the antisense mismatch primer 1977–1953 *Ssp*I (5′-GCC ATA ATT GAA ATA TTT AAC AGT C). A second fragment was derived from the PCR amplification of pMSMΔEnv2 with the antisense primer 2470–2450 (5′-CC TAT AGC TTT ATG TCC GCA G) and the sense mismatch primer 1953–1977 *Ssp*I (5′-G ACT GTT AAA TAT TTC AAT TAT GGC). These fragments were digested with *Ssp*I, ligated, and then reamplified with the sense primer 1465–1485 and the antisense primer 2470–2450. The amplified fragment was digested with *Spe*I and *Bcl*I, and this 922-bp fragment containing the desired mutations was ligated into pMSMΔEnv2 that had been digested with *Spe*I and *Bcl*I.

pNC2 was created by PCR amplification of pMSMΔEnv2 with the sense primer 1953–1977 and the antisense mismatch primer 2048–2023 *Nde*I (5′-CCT TCC TTT CCA TAT GTC CAA TAG CC). A second fragment was derived from the PCR amplification of pMSMΔEnv2 with the antisense primer 2470–2450 and the sense mismatch primer 2023–2048 *Nde*I (5′-GGC TAT TGG ACA TAT GGA AAG GAA GG). These fragments were digested with *Nde*I and ligated and were then reamplified with the sense primer 1465–1485 and the antisense primer 2470–2450. The amplified fragment was digested with *Spe*I and *Bcl*I, and this 922-bp fragment containing the desired mutations was ligated into pMSMΔEnv2 that had been digested with *Spe*I and *Bcl*I. pNC12 was created by the same method as pNC2, except that pNC1 was used as the PCR template.

pΔCA was generated by creating an *Nsi*I (nucleotide [nt] 1251) to *Pst*I (nt 1419) deletion in pMSMΔEnv2. This deletion is identical to the deletion in pdl.NsiPst (previously described [76]).

pGEM(600-900) was generated by PCR amplification of pMSMΔEnv2 with the sense mismatch primer 587–610 *Bam*HI (5′-ACTAGAGATGGATCCGAC CCTTTT) and the antisense mismatch primer 911–888 *Xho*I (5′-AGCTCCCT GCTCGAGCATACTATA). The amplified fragment was digested with *Bam*HI and *Xho*I, and the resulting 300-bp fragment was ligated into pGEMllzf(−) that had been digested with *Bam*HI and *Xho*I. pGEM(600-900) has been previously described (56).

Isolation of cytoplasmic RNA and protein. Cytoplasmic protein and RNA were isolated from a 100-mm-diameter plate of cells by first washing the cells with phosphate-buffered saline (PBS) and then scraping the cells into 1 ml of PBS. The cells were then pelleted by centrifugation for 5 min at 6,000 rpm ($2,200 \times g$). The supernatant was then removed, and the cells were lysed in 0.5 ml of Nonidet P-40 lysis buffer (10 mM Tris [pH 7.5]–10 mM NaCl–3 mM $MgCl_2$–0.5% [wt/vol] Nonidet P-40). The lysate was incubated on ice for 10 min and then centrifuged for 5 min at 6,000 rpm in a microcentrifuge ($2,200 \times g$) to pellet nuclei. The supernatant (cytoplasmic fraction) was removed and used for protein analysis and as a source of cytoplasmic RNA.

RNA was purified from the cytoplasmic fraction by incubation in the presence of proteinase K (Boehringer-Mannheim Biochemicals [BMB]) (500 μg/ml) and 1% sodium dodecyl sulfate (SDS) for 30 min at 37°C. This mixture was then phenol-chloroform extracted, and the nucleic acid was ethyl alcohol (EtOH) precipitated in the presence of 0.3 M sodium acetate. The nucleic acid was then incubated in DNase treatment buffer (50 mM Tris [pH 7.5]–10 mM $MgCl_2$–1 mM dithiothreitol–400 U of RNasin ribonuclease inhibitor (Promega, Madison, Wis.) per ml–100 U of RNase-free DNase I [BMB] per ml) for 30 min at 37°C. Following DNase treatment, the nucleic acid was again phenol-chloroform extracted and EtOH precipitated. The RNA was then resuspended in H_2O, and its concentration was determined by optical density. The RNA was stored at −70°C until further analysis.

Isolation of virion-associated RNA and protein. Virion-associated protein and nucleic acid was isolated by first centrifuging media (30 ml) from three 100-mm-diameter plates of transfected cells at $1,800 \times g$ for 10 min. The supernatant was then transferred to a fresh tube and centrifuged again. The virus was concentrated from the clarified media by centrifugation through a 5-ml cushion consisting of 20% (wt/vol) sucrose-TSE (10 mM Tris [pH 7.5]–100 mM NaCl–1 mM EDTA) for 2 h at 25,000 rpm ($83,000 \times g$) in an SW28 rotor. The virus pellet was then resuspended in 0.5 ml of PK buffer (50 mM Tris [pH 7.5]–100 mM NaCl–10 mM EDTA–1% SDS), and 50 μl was removed and stored at −20°C for subsequent protein analysis. Proteinase K (500 μg/ml) was added to the remaining viral lysate and incubated at 37°C for 30 min. Following this incubation, the nucleic acid was phenol-chloroform extracted and EtOH precipitated in the presence of 20 μg of *Escherichia coli* tRNA. The nucleic acid pellet was resuspended and incubated in DNase treatment buffer for 30 min at 37°C. The nucleic acid was again phenol-chloroform extracted and EtOH precipitated. The RNA pellet was then resuspended in H_2O and stored at −70°C until further analysis.

Western blot analysis. Cytoplasmic (1/10 plate equivalent) or virion-associated (1/3 plate equivalent) protein was suspended in protein loading buffer (10 mM Tris [pH 6.8]–2% SDS–10% glycerol–5 mg of dithiothreitol per ml–0.04% bromphenol blue). Protein samples were subjected to SDS-polyacrylamide gel electrophoresis (PAGE) analysis (10% acrylamide; ratio of bisacrylamide to acrylamide, 29:1) at a constant current of 40 mA for 4 to 6 h (47). Following electrophoresis, proteins were transferred to a nitrocellulose membrane in a Bio-Rad trans-blot cell with Tris–glycine buffer (25 mM Tris–180 mM glycine) at 250 mA for 15 to 18 h at 4°C. Following transfer, the nitrocellulose membrane was rinsed for 5 min in PBS and then incubated for 1 h at room temperature in blocking buffer (PBS containing 5% dry milk and 3% bovine serum albumin). Following blocking, the membrane was incubated for 1 h in antibody incubation buffer (PBS containing 5% dry milk and 1% bovine serum albumin) and a 1/200 dilution of a rabbit anti-Gag serum. This anti-Gag serum was generated in our laboratory by the injection of bacterium-expressed, histidine-tagged Gag protein into rabbits. Following incubation with this primary antibody, membranes were rinsed five times over a period of 30 min with PBS containing 0.05% Tween 20.

The membrane was then incubated in antibody incubation buffer containing a ^{35}S-conjugated donkey anti-rabbit antibody (catalog no. SJ434; Amersham) at a concentration of 0.2 μl/ml (vol/vol) for 1 h. Membranes were again rinsed as described above, dried, and subjected to phosphorimage analysis (model 425S; Molecular Dynamics, Sunnyvale, Calif.).

RNase protection analysis. Antisense riboprobes for RNase protection analysis were transcribed with T7 RNA polymerase (New England Biolabs). The template used for transcription was pGEM(600-900) that had been linearized with *Hin*dIII, proteinase K treated, phenol-chloroform extracted, and EtOH precipitated. Approximately 2.0 μg of template DNA was incubated at 37°C for 30 min in a 20-μl reaction volume under the following buffer conditions: 40 mM Tris (pH 8.0), 10 mM dithiothreitol, 6 mM $MgCl_2$, 2 mM spermidine, 2 U of RNasin ribonuclease inhibitor (Promega) per ml, 400 μM (each) recombinant ATP (rATP), rGTP, and rUTP, 20 μM rCTP, and 50 μCi of [α-^{32}P]CTP (800 Ci/mmol; 20 mCi/ml; catalog no. PB20382; Amersham). Following transcription, 10 U of RNase-free DNase I (BMB) was added and this mixture was incubated at 37°C for 15 min to degrade the DNA template. Unincorporated nucleotides were removed by passing the transcription reaction mixture over a Quick Spin Sephadex G-50 column (BMB) according to the manufacturer's directions.

Ten micrograms of cytoplasmic RNA or 1 plate equivalent of virion-associated RNA was mixed with 10^6 cpm (approximately 200 fmol) (determined by Cerenkov counting) of riboprobe. These RNAs were then EtOH precipitated and resuspended in 30 μl of hybridization buffer {50 mM PIPES [piperazine-*N*,*N*′-bis(2-ethanesulfonic acid)] (pH 6.8), 80% formamide, 400 mM NaCl, 1 mM EDTA}, heated to 95°C for 2 min, and then incubated at 50°C for 15 to 20 h. Following hybridization, the mixture was incubated at room temperature for 1 h and then brought to a volume of 300 μl with RNase digestion buffer (10 mM Tris [pH 7.5]–300 mM NaCl–5 mM EDTA–2 μg of RNase T_1 per ml–10 μg of RNase A per ml). This mixture was then incubated at 37°C for 30 min. The RNase digestion procedure was terminated by the addition of SDS and proteinase K to final concentrations of 1% and 500 μg/ml, respectively. The RNA was then phenol-chloroform extracted and EtOH precipitated along with 20 μg of *E. coli* tRNA.

Pellets were resuspended in 10 μl of RNA loading buffer (80% formamide–10 mM EDTA–0.1% bromphenol blue–0.1% xylene cyanole) and heated to 95°C for 2 min. This mixture was then subjected to PAGE (5% acrylamide [ratio of bisacrylamide to acrylamide, 29:1]–8 M urea–10 mM Tris–10 mM boric acid–2 mM EDTA). DNA molecular weight markers were generated by α-^{32}P[dCTP] end labeling with the Klenow fragment of the plasmid pGEM11Zf(−) (Promega) that had been digested with *Hpa*II. Following electrophoresis, gels were dried under vacuum at 80°C for 2 h. The dried gels were then subjected to phosphorimage analysis.

RESULTS

Analysis of RNA encapsidation by NC mutants. To further characterize the role of each of the Cys-His boxes of the HIV-1 NC protein in RNA encapsidation, a series of mutant virus expression plasmids derived from the WT plasmid pMSMΔEnv2 were constructed (previously described [56]) (Fig. 1A). pMSMΔEnv2 is a derivative of the replication competent proviral clone pNL4-3 (1) that contains both a deletion within the *env* gene and a point mutation that creates a premature stop codon within the *env* gene. Since the *env* gene product is not required for either virus particle production (36) or RNA encapsidation (39, 61, 70), pMSMΔEnv2 can be considered WT for RNA encapsidation and will be referred to as pWT throughout the remainder of the text.

Three HIV-1 expression plasmids that contain mutations which disrupt the Cys-His boxes of the NC protein were constructed (Fig. 1B). pNC1 contains mutations that create cysteine-to-tyrosine substitution mutations at both the first and second cysteine residues of Cys-His box 1 of the NC protein. Similarly, pNC2 contains mutations that create cysteine-to-tyrosine substitution mutations at both the first and second cysteine residues of Cys-His box 2 of the NC protein. pNC2 also contains mutations that create a lysine-to-threonine substitution mutation at amino acid position 38 of NC. pNC12 combines the mutations of both pNC1 and pNC2.

The WT and mutant virus expression plasmids were transfected into 293 cells, a transformed primary embryonic human kidney cell line (29). Cytoplasmic and virion-associated fractions were collected as described in Materials and Methods. Western blot analysis of cytoplasmic protein with Gag antiserum indicated that cells transfected with mutant virus expression plasmids pNC1, pNC2, or pNC12 (Fig. 2A, lanes 2 to 4, respectively) produced similar levels of cytoplasmic Gag protein compared to cells transfected with pWT (Fig. 2A, lane 1). Moreover, cytoplasmic Gag protein expressed from pNC1, pNC2, or pNC12 (Fig. 2A, lanes 2 to 4) exhibited a pattern of proteolytic processing similar to that of pWT (Fig. 2A, lane 1).

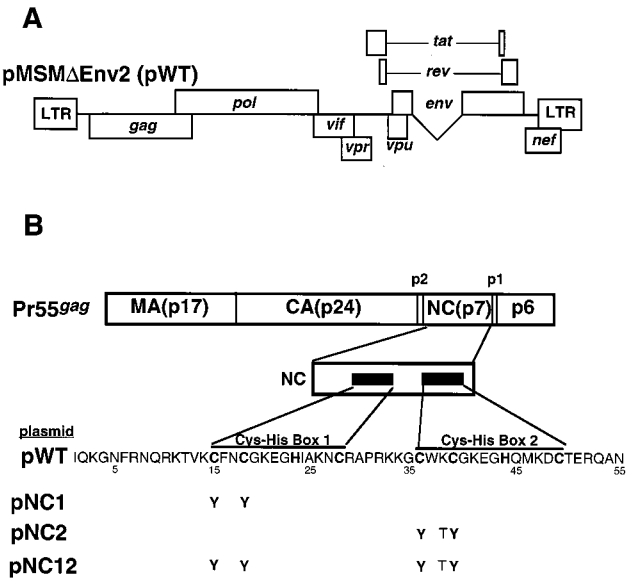

FIG. 1. Diagram of pMSMΔEnv2, protein domains of the Gag polyprotein precursor, and the amino acid sequence of WT and mutant HIV-1 NC proteins. (A) Diagram of virus expression plasmid pMSMΔEnv2 (previously described [56]), referred to as pWT in the text. This plasmid was derived from the replication-competent proviral clone NL4-3 (1) and contains an in-frame premature stop codon at bp 6359 as well as a deletion from bp 6365 to 7252 within the *env* gene. (B) Protein domains of Pr55^{gag}, the amino acid sequence of WT HIV-1 NC, and the substitution mutations present in the mutant NC protein generated by the mutant virus expression plasmids. The Gag polyprotein precursor contains the MA(p17), CA(p24), NC(p7), and p6 protein domains as well as the p2 and p1 spacer peptides. The NC protein of HIV-1 is 55 amino acids in length and contains two Cys-His box motifs located at amino acid positions 15 through 28 and 36 through 49. The cysteine and histidine residues involved in the coordination of Zn^{2+} are in large type (pWT). pNC1 contains mutations that create cysteine-to-tyrosine substitution mutations at amino acids 15 and 18 of the NC protein domain. pNC2 contains mutations that create cysteine-to-tyrosine substitution mutations at amino acids 36 and 39 of the NC protein domain as well as lysine-to-threonine substitution mutations at amino acid 38 of NC. pNC12 contains the mutations that create the six substitution mutations from both pNC1 and pNC2.

Western blot analysis of virion-associated Gag protein indicated that the amount of virus particles produced from pNC1, pNC2, or pNC12 (Fig. 2B, lanes 6 to 8) was similar to the number produced from pWT (Fig. 2B, lane 5). However, disruption of the first Cys-His box or both Cys-His boxes reduced the efficiency of proteolytic processing in virus particles, as evidenced by the increased accumulation of processing intermediates (Fig. 2B, compare lanes 6 and 8 with lane 5).

To determine the efficiency of RNA encapsidation by the NC Cys-His box mutant virus, quantitative RNase protection was used to measure total cytoplasmic and virion-associated RNA produced from 293 cells transfected with WT or mutant virus expression plasmids. The antisense riboprobe used in the RNase protection analysis spans the major subgenomic splice donor, allowing for the distinction between genomic and subgenomic viral RNA (Fig. 3A). RNase protection analysis indicated that the relative amount of genomic and subgenomic viral RNA within the cytoplasm of transfected cells was similar

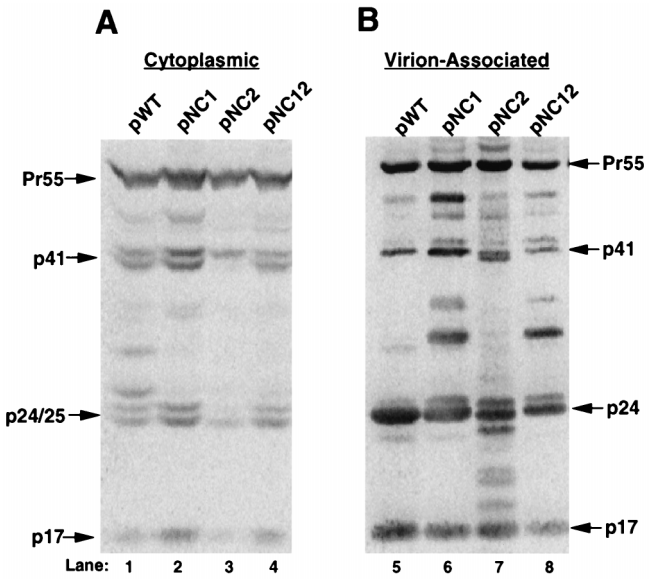

FIG. 2. Western blot analysis of cytoplasmic and virion-associated Gag protein isolated from 293 cells transfected with WT and mutant NC virus expression plasmids. Cytoplasmic protein lysate or virion-associated protein was subjected to SDS-PAGE through a 10% polyacrylamide gel, followed by Western blot analysis with an anti-Gag serum. A ^{35}S-conjugated antibody and phosphorimage analysis were used to visualize Gag protein. Viral protein products are identified by arrows and approximate molecular weight. The relative amount of Gag protein was determined by comparison with a standard curve derived from serial dilutions of Gag protein (data not shown). Phosphorimage analysis of Western blots with serial dilutions of Gag protein indicated that this type of analysis is within the linear range of the assay. (A) Representative Western blot analysis of cytoplasmic protein isolated from 293 cells transfected with pWT, pNC1, pNC2, and pNC12 (lanes 1 to 4, respectively). Lysate from 1/10 plate equivalent was analyzed. (B) Representative Western blot analysis of virion-associated protein isolated from the media of 293 cells transfected with pWT, pNC1, pNC2, and pNC12 (lanes 5 to 8, respectively). Approximately one-third plate equivalent of virion-associated Gag protein was analyzed.

for WT (Fig. 3B, lane 1) and mutant viruses (Fig. 3B, lanes 2 to 4). Subgenomic RNA made up about 40% of the total cytoplasmic viral RNA in each case (Table 1). As expected, the mutations introduced into the NC protein domain did not significantly affect the overall amount of cytoplasmic viral RNA expressed or the extent of the splicing of viral RNA at the major subgenomic splice donor.

The relative amount of viral RNA encapsidated by WT and mutant viruses was determined by RNase protection analysis. Since the amount of viral protein for each sample was similar (Fig. 2B, lanes 5 to 8), the amount of genomic RNA, as determined by quantitative RNase protection analysis, is indicative of the efficiency of genomic RNA encapsidation. RNase protection analysis of cytoplasmic and virion-associated RNA is shown in Fig. 3C, and the results of several independent experiments are summarized in Table 1. NC1 virus was reduced in RNA encapsidation to about 19% of the WT level (Fig. 3C, compare lanes 5 and 6, and Table 1), suggesting that the first Cys-His box of the NC protein is important for efficient genomic RNA encapsidation. NC2 virus was also reduced in RNA encapsidation, but only to about 73% of the WT level (Fig. 3C, compare lanes 5 and 7, and Table 1). In the case of NC12 virus, in which mutations were introduced into both Cys-His boxes, the efficiency of genomic RNA encapsidation was reduced to about 7% of the WT level (Fig. 3C, compare lanes 5 and 8, and Table 1). Taken together, these data suggest that both Cys-His boxes of HIV-1 contribute to efficient genomic RNA encapsidation but that the first is more important than the second for efficient encapsidation of genomic RNA into assembling virus particles.

Mutations in the first Cys-His box of NC result in an increase in encapsidation of subgenomic RNA. In WT HIV-1, subgenomic RNA makes up only about 2% of the encapsidated viral RNA. However, NC1 and NC12 mutant viruses encapsidated subgenomic RNA with a markedly increased efficiency (54 and 52% of the total encapsidated viral RNA, respectively) (Fig. 3C and Table 1). Furthermore, this increase in the percentage of subgenomic RNA in virus particles represented an actual increase in the encapsidation of subgenomic RNA and not merely a decrease in the encapsidation of genomic RNA. These data indicate that Cys-His box 1 of the HIV-1 NC protein is important not only for the efficient encapsidation of genomic RNA but also for the specific recognition of genomic RNA and the concomitant exclusion of subgenomic RNA during the assembly of virus particles. Mutations in the second Cys-His box only marginally increased the amount of subgenomic RNA found to be associated with NC2 virus particles compared to the amount associated with WT virus particles (Table 1 and Fig. 3C, compare lanes 5 and 7).

Composite virus particles composed of both WT and mutant NC proteins encapsidate RNA with a similar efficiency and specificity as WT particles. If multiple functional NC domains on separate Gag molecules are required for encapsidation, coexpression of NC1 or NC12 mutant Gag protein with WT Gag protein might be expected to dominantly interfere with RNA encapsidation mediated by WT Gag. Conversely, if only a subset of Gag molecules in the viral capsid need to contain a functional NC domain, then coexpression of NC1 or NC12 mutant Gag with WT Gag protein might not significantly affect encapsidation. Thus, 293 cells were cotransfected with equimolar amounts of WT and mutant virus expression plasmids. Western blot analysis indicated that similar amounts of virus were released from cells cotransfected with WT and NC mutant plasmids compared to the amount released from cells transfected with WT plasmid alone (Fig. 4A, compare lane 1 to lanes 2 to 4). Interestingly, RNase protection analysis indicated that virus generated from cells coexpressing WT Gag and any of the mutant NC Gag proteins retained the ability to efficiently encapsidate genomic viral RNA (Fig. 5A, lanes 1 to 4). A summary of the relative genomic RNA encapsidation efficiency from several independent experiments is shown in the bottom panel of Fig. 5A. Moreover, the composite virus particles excluded subgenomic viral RNA with an efficiency similar to that of the WT virus (Fig. 5A).

To further examine the encapsidation efficiency of heterogeneous virus particles, the encapsidation efficiency of virus particles produced from the coexpression of various combinations of the NC mutants was determined. As expected, Western blot analysis indicated that similar amounts of virus were released from cells cotransfected with the various combinations of NC mutant expression plasmids (Fig. 4B, lanes 5 to 8). RNase protection analysis indicated that virus produced from cells cotransfected with pNC2 and either pNC1 or pNC12 encapsidated genomic RNA with a relatively high efficiency (approximately 74 or 89% that of WT, respectively) (Fig. 5B, compare lanes 7 and 9 with lane 6). A summary of the relative genomic RNA encapsidation efficiencies from several independent experiments is shown in the bottom panel of Fig. 5B. In contrast, virus produced from cells cotransfected with pNC1 and pNC12 had a drastically reduced ability to encapsidate genomic RNA, having a relative RNA encapsidation level of approximately 10% compared to that of WT (Fig. 5B, compare lanes 6 and 8). Thus, these data are in concordance with the idea that RNA encapsidation requires that only a subset of the

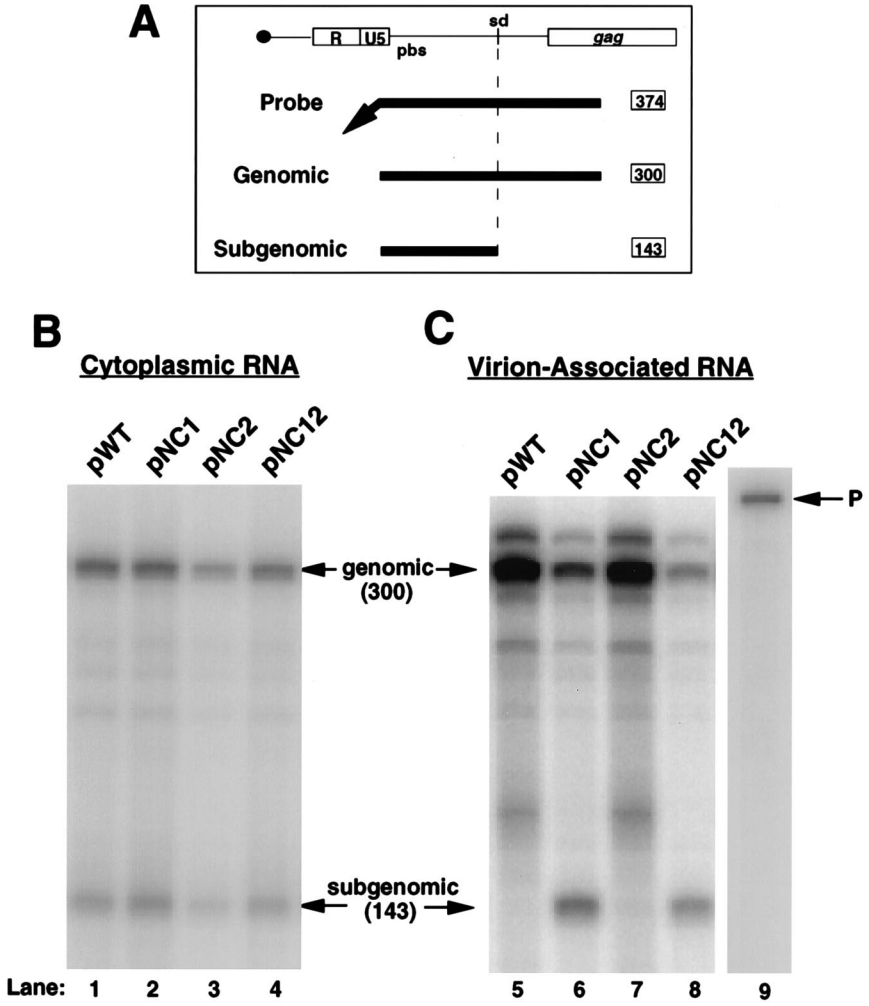

FIG. 3. RNase protection analysis of cytoplasmic and virion-associated RNA isolated from 293 cells transfected with WT and mutant NC virus expression plasmids. (A) Region of complementarity between the antisense riboprobe and the 5′ region of HIV-1 RNA. The probe is 374 nt in length. The diagnostic fragment for full-length genomic RNA is 300 nt in length, and the diagnostic fragment for subgenomic RNA that is spliced at the major subgenomic splice donor is 143 nt in length. (B and C) Riboprobe was generated by in vitro transcription with T7 RNA polymerase of *Hin*dIII-linearized pGEM(600-900). Transcription reactions were performed in the presence of [^{32}P]CTP. The probe was used in RNase protection analysis as described in Materials and Methods. The protected fragments resulting from RNase protection analysis were resolved on a 5% polyacrylamide-8 M urea gel. The gel was dried, and radiolabeled probe was visualized by phosphorimage analysis. The diagnostic bands for genomic and subgenomic RNA are indicated (arrows). Undigested probe (P) is shown in lane 9. (B) Ten-microgram amounts of total cytoplasmic RNA isolated from cells transfected with pWT, pNC1, pNC2, and pNC12 (lanes 1 to 4, respectively) were analyzed by RNase protection. (C) Virion-associated RNA isolated from the media of approximately one plate equivalent of cells transfected with pWT, pNC1, pNC2, and pNC12 (lanes 5 to 8, respectively) was analyzed by RNase protection.

Gag proteins in a virus particle contain a WT copy of Cys-His box 1. The absence of a WT copy of Cys-His box 1 also results in a higher amount of subgenomic RNA becoming associated with virus particles (Fig. 5B, lane 8). These results, taken together, provide additional evidence that Cys-His box 1 is more important than Cys-His box 2 in genomic RNA encapsidation and in the specificity of genomic RNA encapsidation.

To test further the idea that successful RNA encapsidation requires only a partial complement of WT NC protein, various ratios of WT and NC mutant virus expression plasmids were cotransfected into cells and the resulting virus particles were analyzed for the ability to encapsidate viral RNA. Again, Western blot analysis indicated that at all ratios of transfected DNA tested, the amount of virus released was similar (Fig. 6). The efficiency of genomic RNA encapsidation remained relatively high, even at WT-to-NC1 plasmid ratios of up to 1:20 (Fig. 7A). A summary of the relative genomic RNA encapsidation

TABLE 1. Summary of analysis of cytoplasmic and virion-associated RNA from 293 cells transfected with WT and NC mutant virus expression plasmids[a]

Virus	Mean ± SD of cytoplasmic RNA	Mean ± SD of virion-associated RNA	
	% Subgenomic[b]	Relative genomic	% Subgenomic[b]
WT	39 ± 3	1.0	2 ± 0.7
NC1	34 ± 2	0.19 ± 0.04	54 ± 5
NC2	44 ± 3	0.73 ± 0.08	8 ± 4
NC12	36 ± 4	0.07 ± 0.01	52 ± 5

[a] Cytoplasmic and virion-associated RNAs were isolated as described in Materials and Methods and in the legend for Fig. 3.

[b] Calculations of percentages of cytoplasmic subgenomic RNA and virion-associated subgenomic RNA were corrected for the differences in protected probe lengths. Values reported were derived from at least three independent experiments.

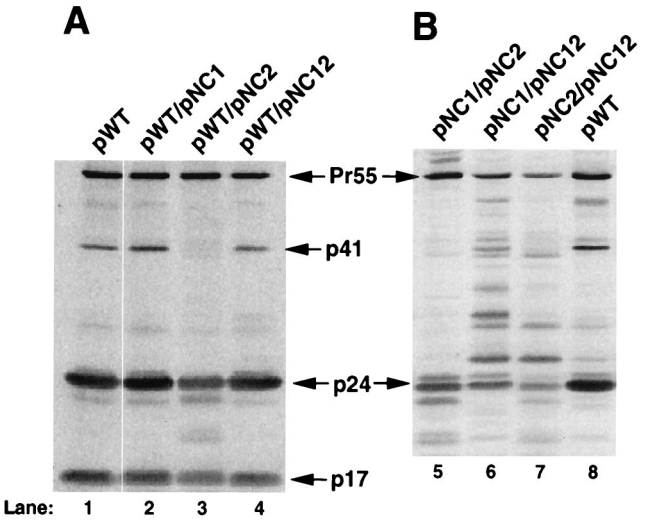

FIG. 4. Western blot analysis of virion-associated protein isolated from the media of 293 cells cotransfected with equimolar amounts of WT and NC mutant plasmids or combinations of the NC mutant plasmids. Western blot analysis was performed as described in the legend for Fig. 2. (A) Representative Western blot analysis of virion-associated protein isolated from the media of approximately one-third plate equivalent of cells transfected with pWT (lane 1) or cotransfected with pWT and each of the NC mutant plasmids (lanes 2 to 4). (B) Representative Western blot analysis of virion-associated protein isolated from the media of approximately one-third plate equivalent of cells transfected with pWT (lane 8) or cotransfected with combinations of each of the NC mutant plasmids (pNC1/pNC2, pNC1/pNC12, and pNC2/pNC12) (lanes 5 to 7, respectively).

efficiencies from several independent experiments is shown in Fig. 7B. Analysis of virus produced from cells cotransfected with various ratios of pWT and pNC12 virus expression plasmids indicated that near-WT levels of genomic RNA encapsidation can also occur at ratios of WT to NC12 plasmids as high as 1:20 (Fig. 7A). Finally, virus produced from cells cotransfected with various ratios of pWT and pNC2 virus expression plasmids retained WT levels of genomic RNA encapsidation up to WT-to-NC2 ratios of 1:20 (Fig. 7A, lanes 7 to 9). This last observation was not surprising given that homogeneous NC2 particles retain a near-WT level of genomic RNA encapsidation (Fig. 3C and Table 1).

The relative amount of subgenomic RNA associated with virus particles is also shown in Fig. 7A. As the ratio of WT to NC1 or WT to NC12 was increased, the amount of subgenomic RNA that was associated with virus particles also increased (Fig. 7B), indicating that as the amounts of NC1 and NC12 mutant proteins increased, the ability of these heterogeneous virus particles to discriminate between genomic and subgenomic RNA was reduced.

Since the primary Gag gene products expressed from pNC1, pNC12, and pWT were indistinguishable by Western blot analysis, it was difficult to directly compare the levels of Gag protein expression in the cotransfection experiments. To directly determine whether the various transfection conditions were actually producing virus particles that contained the predicted types and amounts of Gag proteins, a virus expression plasmid containing a 168-bp, in-frame deletion within the *gag* gene was used (Fig. 8A). This deletion results in the production of a Gag precursor that lacks 56 amino acids of the CA protein domain, and a similar mutant has been previously described (76). Previous characterization of pΔCA indicated that it was competent for virus particle production and, as shown below, ΔCA virus particles are capable of efficient RNA encapsidation.

Western blot analysis of virion-associated Gag protein isolated from cells transfected with various ratios of pΔCA and pNC12 is shown (Fig. 8B). As expected, transfection of pΔCA resulted in the production of virus that contained a smaller Gag precursor (Pr49ΔCA) than did virus produced from pNC12 (Pr55). The ΔCA virus also contained a smaller mature CA protein (p18ΔCA) than the NC12 virus did (p24) (Fig. 8B). As the ratio of pΔCA:pNC12 was decreased (Fig. 8B, lanes 2 to 5), the levels of Pr55 increased, while the levels of Pr49ΔCA decreased. At the same time, the levels of p24 increased, while the levels of p18ΔCA decreased. Quantitative phosphorimage analysis indicated that the population of virus particles produced in this experiment mirrors the relative amount and types of virus expression plasmids used in these cotransfections.

RNase protection analysis was performed to measure the RNA encapsidated by composite virus particles composed of ΔCA and NC12 Gag protein. The amount of virion-associated RNA paralleled that of particles made up of WT and NC12 Gag protein (Fig. 7 and 8C). Moreover, even though the level

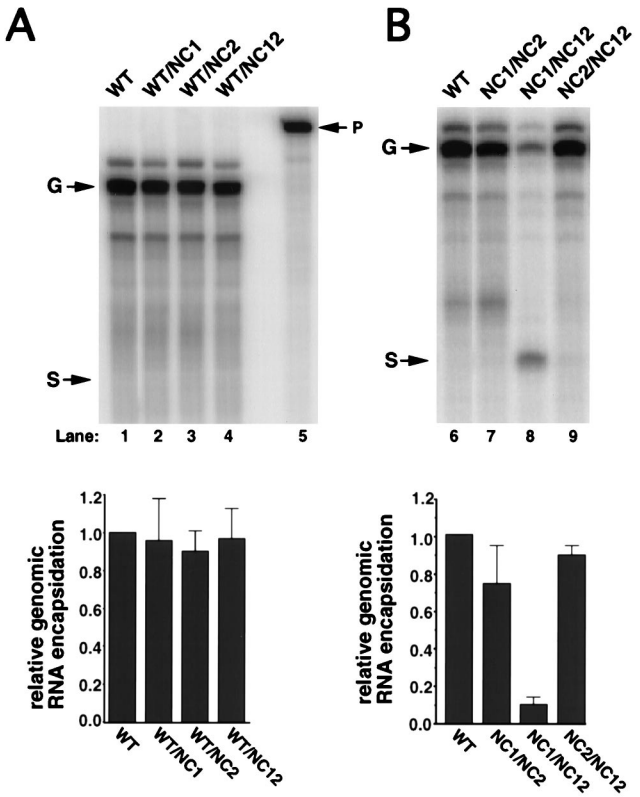

FIG. 5. RNase protection analysis of virion-associated RNA isolated from the media of 293 cells cotransfected with WT and mutant NC plasmids or combinations of NC mutant plasmids. RNase protection analysis was performed as described in the legend for Fig. 3. The riboprobe is shown in lane 5 (P). The diagnostic fragments for genomic (G) and subgenomic (S) RNAs are indicated (arrows). An average genomic RNA encapsidation efficiency determined from the results of several independent experiments is represented by bar graphs. The standard deviation (SD) from the mean is represented by error bars. The relative genomic encapsidation efficiency for pWT was normalized to 1.0 for each experiment. (A) Representative RNase protection analysis of virion-associated RNA isolated from the media of cells transfected with pWT (lane 1) or cotransfections of pWT with pNC1, pNC2, and pNC12 (lanes 2 to 4, respectively). The total amount of DNA transfected was kept constant. (B) Representative RNase protection analysis of virion-associated RNA isolated from the media of cells transfected with pWT (lane 6) or cotransfections of pNC1/pNC2, pNC1/pNC12, and pNC2/pNC12 (lanes 7 to 9, respectively). The total amount of DNA transfected was kept constant.

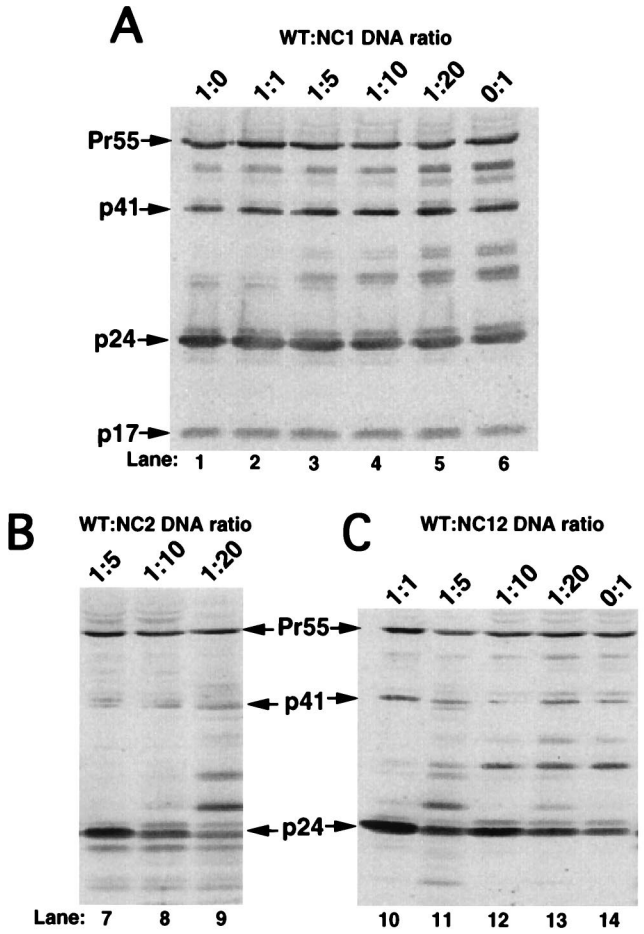

FIG. 6. Western blot analysis of virion-associated Gag protein isolated from the media of 293 cells cotransfected with varying ratios of WT to NC mutant plasmid. Western blot analysis was performed as described in the legend for Fig. 2. For each ratio, the total amount of virus expression plasmid transfected was kept constant. (A) Representative Western blot analysis of virion-associated Gag protein isolated from the media of cells cotransfected with WT to NC1 plasmid ratios of 1:0, 1:1, 1:5, 1:10, 1:20, and 0:1 (lanes 1 to 6, respectively). (B) Representative Western blot analysis of virion-associated Gag protein isolated from the media of cells cotransfected with WT to NC2 plasmid ratios of 1:5, 1:10, and 1:20 (lanes 7 to 9, respectively). (C) Representative Western blot analysis of virion-associated Gag protein isolated from the media of cells cotransfected with WT to NC12 plasmid ratios of 1:1, 1:5, 1:10, 1:20, and 0:1 (lanes 10 to 14, respectively).

of WT ΔCA protein was significantly reduced as the ratio of pΔCA to pNC12 was decreased, the level of RNA encapsidation remained relatively high (Fig. 8C). This result demonstrated that WT Gag protein, expressed from pΔCA, can *trans*-complement mutant Gag protein, expressed from pNC12, resulting in efficient RNA encapsidation.

Composite virus particles composed of both WT and mutant NC proteins can replicate. Since virus particles produced from cotransfection of cells with pWT and any of the NC mutant expression plasmids retained the ability to efficiently encapsidate genomic RNA, it was of interest to determine whether these particles could replicate. To test for replication, virus particles were produced by cotransfection of 293 cells with the various HIV-1 expression plasmids and a plasmid that expresses an amphotropic murine leukemia virus envelope glycoprotein (pSV-A-MLV) (63). Virus particles were then assayed for infectivity with CD4-LTR/β-Gal indicator cells as previously described (23, 43). Virus produced from transfection of cells with pWT produced approximately 8×10^3 blue cells/ml, while neither pNC1, pNC2, nor pNC12 produced detectable numbers of blue cells (Table 2). Interestingly, cotransfection of cells with pWT and either pNC1, pNC2, or pNC12 yielded significant amounts of infectious virus (Table 2). Finally, cotransfection of various combinations of the NC mutants produced significantly lower numbers of infectious viruses than did WT (Table 2). These results indicated that a full complement of WT NC is not required for infectivity of virus particles.

DISCUSSION

We have further characterized the role of the NC protein in the efficient and specific encapsidation of HIV-1 genomic RNA. Our data suggest that Cys-His box 1 is more important for RNA encapsidation than Cys-His box 2, consistent with previous reports (25, 27). Our finding that composite particles must contain at least some copies of WT Cys-His box 1 further suggests that Cys-His box 1 is more important than Cys-His box 2 in HIV-1 RNA encapsidation. The observation that HIV-1 particles containing mutations in Cys-His box 1 have a reduced ability to specifically encapsidate genomic RNA over subgenomic RNA is consistent with the work of others (8, 79). In contrast, Poon et al. demonstrated that mutations affecting some of the charged amino acids of HIV-1 NC did not lead to an increase in the encapsidation efficiency of subgenomic viral RNA (66).

A subset of the *cis*-acting encapsidation elements present on HIV-1 genomic RNA is also found on subgenomic RNA (56, 58). Also, encapsidation elements described for the avian leukosis viruses are present on both genomic and subgenomic RNAs (38, 44). It is probable that exonic RNA encapsidation elements are capable of promoting suboptimal encapsidation of subgenomic RNA into assembling virus particles, even though they lack intronic encapsidation signals. Along the same lines, reticuloendotheliosis virus vectors containing exonic RNA elements are encapsidated more efficiently than vectors lacking these elements (22). Similarly, HIV-1 and Rous sarcoma virus subgenomic RNAs are encapsidated with high efficiency compared to nonviral RNA (38, 54), and HIV-1 subgenomic RNA is encapsidated more efficiently than nonviral RNA (8). Finally, experiments were performed to measure the encapsidation of highly expressed nonviral RNAs, and it was found that there was not an increase in the encapsidation of these nonviral RNAs by NC1 or NC12 mutant virus (data not shown). These results reinforce the idea that the encapsidation signal is multipartite and that maximal encapsidation requires both exonic and intronic sequences (56).

Since mutations within Cys-His box 1 reduce the ability of the assembling virus particle to discriminate between genomic and subgenomic RNAs it is likely that Cys-His box 1 is required for recognition of a sequence or element derived, at least in part, from the viral intron. Such an RNA element either could be fully contained on the intron of viral RNA or could contribute to the formation of a higher-order structure composed of exonic and intronic sequences. It is interesting that a similar phenotype, a loss in discrimination between the encapsidation of genomic and subgenomic RNAs, has been observed following disruption of stem-loop 3 in the 5′ region of the HIV-1 genome (56) or deletion of HIV-1 intronic sequences (54). We suggest that the recognition of genomic RNA involves interaction between Cys-His box 1 and such a *cis*-acting sequence. An extension of this idea is that other domains of Gag recognize *cis*-acting elements that are located upstream of the major

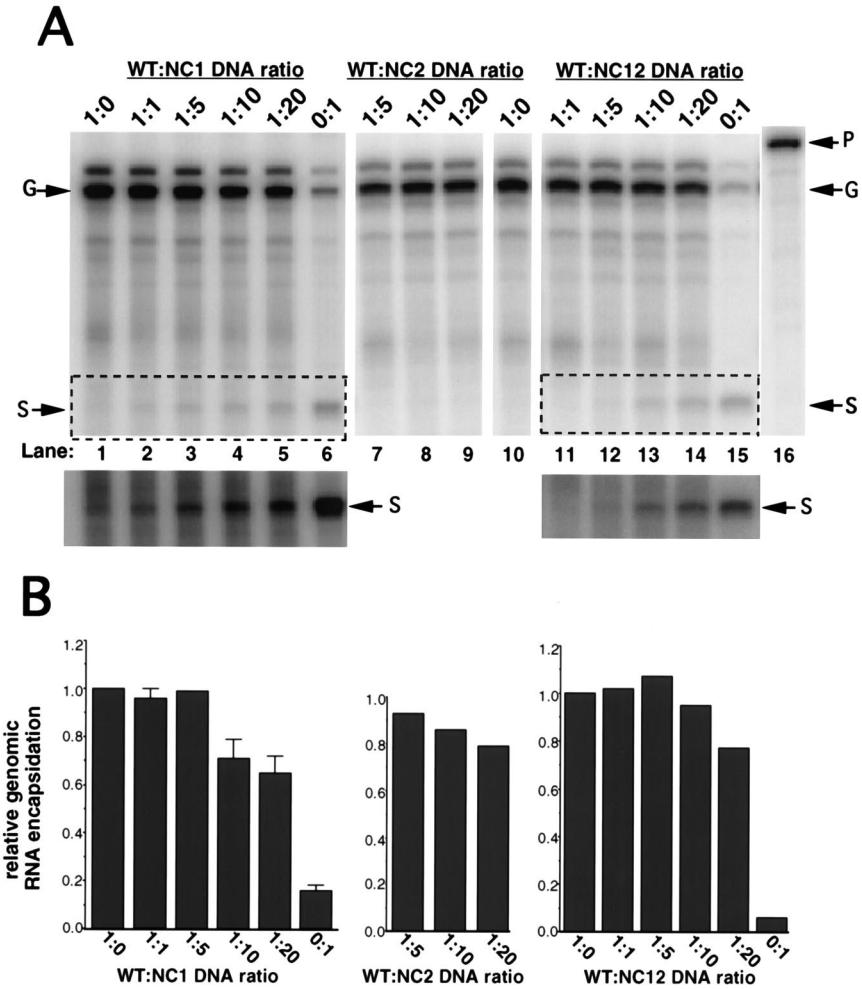

FIG. 7. RNase protection analysis of virion-associated RNA isolated from the media of 293 cells cotransfected with varying ratios of WT to NC mutant plasmids. RNase protection analysis was performed as described in the legend for Fig. 3. The riboprobe is shown in lane 16 (P). Fragments representing genomic (G) and subgenomic (S) RNA are indicated (arrows). (A) Representative RNase protection analysis of virion-associated RNA isolated from the media of cells cotransfected with various ratios of WT to NC mutant plasmids. The plasmids transfected are indicated above the gels, and the ratios of WT to NC mutant plasmids are indicated above each lane. A longer exposure of the boxed regions of the gels is shown below. (B) An average genomic RNA encapsidation efficiency was determined from several independent experiments, and the SD from the mean is represented by error bars. The relative genomic encapsidation efficiency for pWT was normalized to 1.0 for each experiment.

subgenomic splice donor and present on both genomic and subgenomic RNAs (58).

The exact status of the Gag precursor proteins during RNA recognition and encapsidation is unclear. The recognition of genomic RNA may be mediated through a single Gag monomer or by multiple Gag monomers. Virus particles produced by transfection of WT-to-NC mutant DNA ratios as high as 1:20 had encapsidation efficiencies near WT levels. One interpretation of these observations is that a limited number of Gag molecules need to interact with RNA for efficient encapsidation to occur. Since only two RNA molecules are encapsidated into each virus particle, we favor the possibility that very few Gag molecules are required for initial recognition of RNA. However, another possibility is that the WT Gag molecules present in heterogeneous virus particles can act in *trans* to coordinate the formation of multi-Gag complexes composed of both WT and mutant molecules, thus allowing mutant molecules to contribute to RNA recognition and encapsidation. The NC protein of HIV-1 is found associated with viral RNA in mature particles mostly through nonspecific interactions (16). It would be interesting to determine whether NC is still found to be associated with viral RNA in heterogeneous virus particles containing both WT and mutant NC proteins.

Mutations in either Cys-His box 1 or 2 result in a reduction in replication of at least 4 orders of magnitude, while the reduction in RNA encapsidation is only 1 order in magnitude, suggesting that these NC mutations likely affect other roles in viral replication. Other roles that have been attributed to Cys-His boxes include nonspecific coating of RNA to protect the RNA from degradation (49), promotion of DNA strand transfer during reverse transcription, promotion of dimerization of viral RNA, and the annealing of replication primer tRNA to the primer binding site (18, 37, 41, 48, 67, 75). In contrast, heterogeneous particles produced from the cotransfection of WT and any of the NC mutant virus expression plasmids resulted in virus particles capable of highly efficient replication. This result indicates that no step in nucleic acid replication requires a full complement of WT NC.

Mutations in the first Cys-His box resulted in a reduction in proteolytic processing of Gag. Perhaps mutations of Cys-His

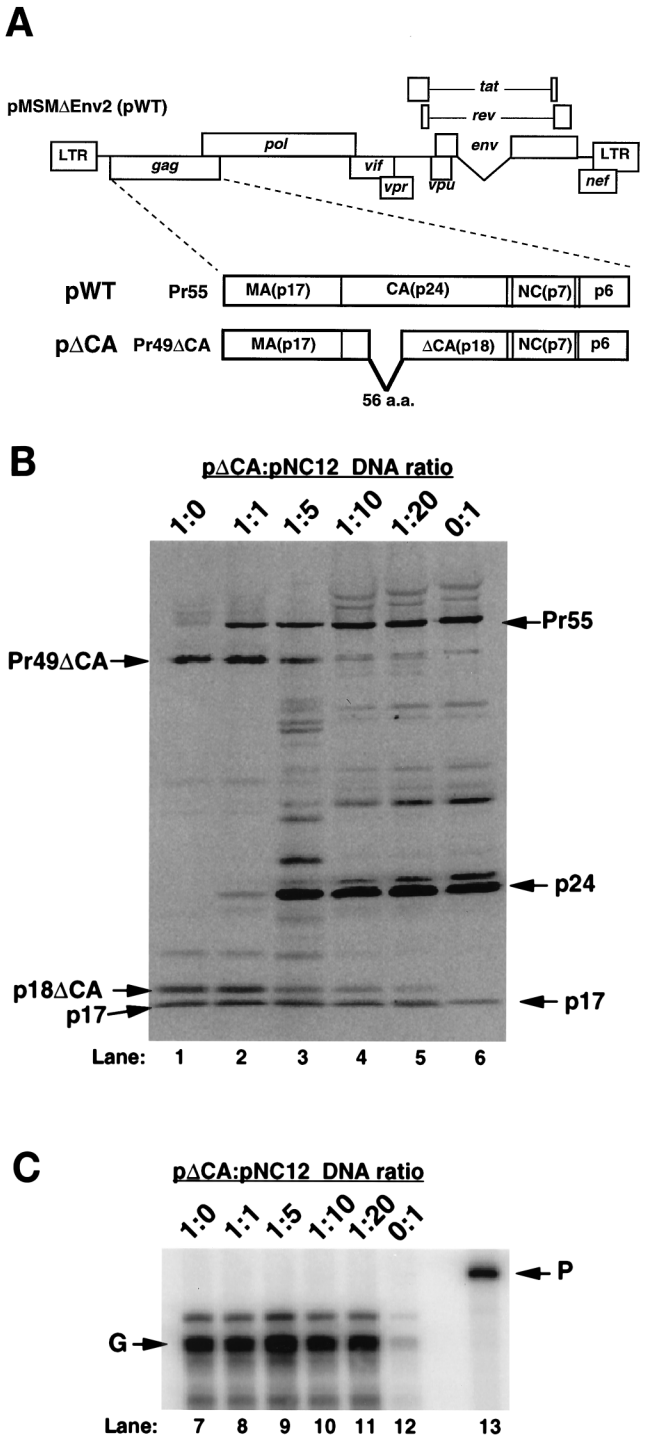

FIG. 8. Diagram of pΔCA and Western blot and RNase protection analysis of 293 cells cotransfected with varying ratios of pΔCA and pNC12. (A) pΔCA contains a 168-nt deletion from *Nsi*I (bp 1251) to *Pst*I (bp 1419). This deletion results in the production of a truncated Gag precursor containing a 56-amino-acid (a.a.) deletion within the CA domain. The Gag precursor produced from pΔCA has an approximate molecular mass of 49 kDa (Pr49ΔCA), and the mature capsid protein produced from pΔCA has an approximate molecular mass of 18 kDa (p18ΔCA). (B) Representative Western blot analysis of virion-associated Gag protein isolated from the media of cells cotransfected with pΔCA to NC12 plasmid ratios of 1:0, 1:1, 1:5, 1:10, 1:20, and 0:1 (lanes 1 to 6, respectively). Western blot analysis was performed as shown in Fig. 2. The predicted protein products from pWT (Pr55, p24, and p17) and from pΔCA (Pr49ΔCA, p18ΔCA, and p17) are indicated (arrows). Phosphorimage analysis indicated that the population of virus particles produced in this experiment mirrored the relative amount and types of virus expression plasmids used in these cotransfections. (C) Representative RNase protection analysis of virion-associated RNA isolated from the media of cells cotransfected with pΔCA to NC12 plasmid ratios of 1:0, 1:1, 1:5, 1:10, 1:20, and 0:1 (lanes 7 to 12, respectively). RNase protection analysis was performed as shown in Fig. 3. Predicted fragments for genomic RNA (G) and undigested probe (P) are indicated.

TABLE 2. Infectivity of NC mutant virus particles and virus particles produced from cotransfection of WT and NC mutations assayed by CD4-LTR/β-Gal indicator cells[a]

Plasmid(s)[b]	Relative no. of blue cell-forming U/ml
pWT	1.0
pNC1	0
pNC2	0
pNC12	0
pWT/pNC1	0.8 ± 0.50
pWT/pNC2	0.3 ± 0.1
pWT/pNC12	0.5 ± 0.3
pNC1/pNC2	0
pNC1/pNC12	0
pNC2/pNC12	0

[a] The CD4-LTR/β-Gal infectivity assay was performed as described in Materials and Methods.

[b] A total of 15 μg of DNA was transfected per plate (7.5 μg of virus expression plasmid[s] and 7.5 μg of the amphotropic envelope expression plasmid, pSV-A-MLV). In the case of cotransfection of virus expression plasmids, 3.75 μg of each plasmid was transfected. Values for relative numbers of blue cell-forming units were normalized to pWT (1.0). The average number of blue cell-forming units for WT was 75,000. The SD from the mean is reported.

box 1 lead to a defect in processing due to a *cis* effect. In other words, when mutations are present in Cys-His box 1, the cleavage sites in the Gag precursor are altered in a way that does not allow efficient processing by the viral protease. However, this defect in processing was not observed in experiments in which NC1 or NC12 mutant Gag molecules were coexpressed with WT Gag (Fig. 4A). This processing defect was not observed in the NC1/NC2 or NC2/NC12 cotransfection experiments either (Fig. 4B). On the surface, these results suggest that a *cis*-acting processing defect can be rescued in *trans* by Gag molecules that can be processed. However, we propose that efficient proteolytic processing requires the encapsidation of viral or cellular RNA. In cases in which a processing defect is observed, the virus particles contain less viral RNA and perhaps less total RNA than do WT virus particles (Fig. 3 and 5). Other reports have also suggested a potential role for RNA during virus particle assembly and maturation. Sheng and Erickson-Viitanen demonstrated that in vitro proteolytic cleavage of p15, the NC-p6^{gag} processing intermediate, by HIV-1 protease is RNA dependent (73). Campbell and Vogt found that efficiency of in vitro assembly of HIV-1-like particles was dramatically increased when RNA was present (12).

If RNA is required for Gag processing, viral RNA per se is probably not required. Western blot analysis from the cytomegalovirus mutant $CMV_{259}\Delta21$ (56), which is deficient in HIV-1 RNA encapsidation due to a *cis*-acting defect, does not exhibit a similar defect in the efficiency of proteolytic processing (data not shown). It is likely that $CMV_{259}\Delta21$ virus particles contain quantities of nonviral RNA sufficient for processing, whereas the *trans*-acting encapsidation mutants, NC1 and

NC12, do not contain enough viral or nonviral RNA for proper maturation.

ACKNOWLEDGMENTS

We thank Michael Havert and Mark Handley for critical reviews of the manuscript, Kate Gerten for technical assistance, and Dan Loeb for helpful discussion.

This work was supported by NIH grant ROI AI 34733. M.D.S. is a Cremer scholar.

REFERENCES

1. **Adachi, A., H. E. Gendelman, S. Koenig, T. Folks, R. Wiley, A. Rabson, and M. A. Martin.** 1986. Production of acquired immunodeficiency syndrome-associated retrovirus in human and nonhuman cells transfected with an infectious molecular clone. J. Virol. **59:**284–291.
2. **Aldovini, A., and M. B. Feinberg.** 1990. Transfection of molecularly cloned HIV-1 genomes, p. 147–175. *In* A. Aldovini and B. D. Walker (ed.), Techniques in HIV research. Stockton Press, New York, N.Y.
3. **Aldovini, A., and R. A. Young.** 1990. Mutations of RNA and protein sequences involved in human immunodeficiency virus type 1 packaging result in production of noninfectious virus. J. Virol. **64:**1920–1926.
4. **Baudin, F., R. Marquet, C. Isel, J. L. Darlix, B. Ehresmann, and C. Ehresmann.** 1993. Functional sites in the 5′ region of human immunodeficiency virus type 1 RNA form defined structural domains. J. Mol. Biol. **229:**382–397.
5. **Berg, J.** 1986. Potential metal-binding domains in nucleic acid binding proteins. Science **232:**485–487.
6. **Berkowitz, R. D., and S. P. Goff.** 1994. Analysis of binding elements in the human immunodeficiency virus type 1 genomic RNA and nucleocapsid protein. Virology **202:**233–246.
7. **Berkowitz, R. D., J. Luban, and S. P. Goff.** 1993. Specific binding of human immunodeficiency virus type 1 *gag* polyprotein and nucleocapsid protein to viral RNAs detected by RNA mobility shift assays. J. Virol. **67:**7190–7200.
8. **Berkowitz, R. D., Å. Ohagen, S. Höglund, and S. P. Goff.** 1995. Retroviral nucleocapsid domains mediate the specific recognition of genomic viral RNAs by chimeric Gag polyproteins during RNA packaging in vivo. J. Virol. **69:**6445–6456.
9. **Bess, J. W. J., P. J. Powell, H. J. Issaq, L. J. Schumack, M. K. Grimes, L. E. Henderson, and L. O. Arthur.** 1992. Tightly bound zinc in human immunodeficiency virus type 1, human T-cell leukemia virus type 1, and other retroviruses. J. Virol. **66:**840–847.
10. **Bowles, N. E., P. Damay, and P. F. Spahr.** 1993. Effect of rearrangements and duplications of the Cys-His motifs of Rous sarcoma virus nucleocapsid protein. J. Virol. **67:**623–631.
11. **Bryant, M., and L. Ratner.** 1990. Myristoylation-dependent replication and assembly of human immunodeficiency virus 1. Proc. Natl. Acad. Sci. USA **87:**523–527.
12. **Campbell, S., and V. M. Vogt.** 1995. Self-assembly in vitro of purified CA-NC proteins from Rous sarcoma virus and human immunodeficiency virus type 1. J. Virol. **69:**6487–6497.
13. **Clavel, F., and J. M. Orenstein.** 1990. A mutant of human immunodeficiency virus with reduced RNA packaging and abnormal particle morphology. J. Virol. **64:**5230–5234.
14. **Clever, J., C. Sassetti, and T. G. Parslow.** 1995. RNA secondary structure and binding sites for *gag* gene products in the 5′ packaging signal of human immunodeficiency virus type 1. J. Virol. **69:**2101–2109.
15. **Dannull, J., A. Surovoy, G. Jung, and K. Moelling.** 1994. Specific binding of HIV-1 nucleocapsid protein to PSI RNA in vitro requires N-terminal zinc finger and flanking basic amino acid residues. EMBO J. **13:**1525–1533.
16. **Darlix, J. L., C. Gabus, M. T. Nugeyre, F. Clavel, and F. Barre-Sinoussi.** 1990. *Cis* elements and *trans*-acting factors involved in the RNA dimerization of the human immunodeficiency virus HIV-1. J. Mol. Biol. **216:**689–699.
17. **Davis, J., M. Scherer, W. P. Tsai, and C. Long.** 1976. Low-molecular-weight Rauscher leukemia virus protein with a preferential binding for single-stranded RNA and DNA. J. Virol. **18:**709–718.
18. **De Rocquigny, H., C. Gabus, A. Vincent, M. C. Fournie-Zaluski, B. Roques, and J. L. Darlix.** 1992. Viral RNA annealing activities of human immunodeficiency virus type 1 nucleocapsid protein require only peptide domains outside the zinc fingers. Proc. Natl. Acad. Sci. USA **89:**6472–6476.
19. **Dorfman, T., J. Luban, S. P. Goff, W. A. Haseltine, and H. G. Gottlinger.** 1993. Mapping of functionally important residues of a cysteine-histidine box in the human immunodeficiency virus type 1 nucleocapsid protein. J. Virol. **67:**6159–6169.
20. **Dupraz, P., S. Oertle, C. Meric, P. Damay, and P.-F. Spahr.** 1990. Point mutations in the proximal Cys-His box of Rous sarcoma virus nucleocapsid protein. J. Virol. **64:**4978–4987.
21. **Dupraz, P., and P.-F. Spahr.** 1992. Specificity of Rous sarcoma virus nucleocapsid protein in genomic RNA packaging. J. Virol. **66:**4662–4670.
22. **Embretson, J. E., and H. M. Temin.** 1987. Lack of competition results in efficient packaging of heterologous murine retroviral RNAs and reticuloendotheliosis virus encapsidation-minus RNAs by the reticuloendotheliosis virus helper cell line. J. Virol. **61:**2675–2683.
23. **Geraghty, R. J., and A. T. Panganiban.** 1993. Human immunodeficiency virus type 1 has a CD4- and envelope glycoprotein-independent function. J. Virol. **67:**4190–4194.
24. **Gheysen, D., E. Jacobs, F. de Foresta, C. Thiriart, M. Francotte, D. Thines, and M. De Wilde.** 1989. Assembly and release of HIV-1 precursor Pr55^{gag} virus-like particles from recombinant baculovirus-infected insect cells. Cell **59:**103–112.
25. **Gorelick, R. J., D. J. Chabot, A. Rein, L. E. Henderson, and L. O. Arthur.** 1993. The two zinc fingers in the human immunodeficiency virus type 1 nucleocapsid protein are not functionally equivalent. J. Virol. **67:**4027–4036.
26. **Gorelick, R. J., L. E. Henderson, J. P. Hanser, and A. Rein.** 1988. Point mutants of Moloney murine leukemia virus that fail to package viral RNA: evidence for specific RNA recognition by a "zinc finger-like" protein sequence. Proc. Natl. Acad. Sci. USA **85:**8420–8424.
27. **Gorelick, R. J., S. M. Nigida, J. R. Bess, L. O. Arthur, L. E. Henderson, and A. Rein.** 1990. Noninfectious human immunodeficiency virus type 1 mutants deficient in genomic RNA. J. Virol. **64:**3207–3211.
28. **Gottlinger, H. G., J. G. Sodrowski, and W. A. Haseltine.** 1989. Role of capsid precursor processing and myristoylation in morphogenesis and infectivity of human immunodeficiency virus type 1. Proc. Natl. Acad. Sci. USA **86:**5781–5785.
29. **Graham, F. L., J. Smiley, W. C. Russell, and R. Nairn.** 1977. Characteristics of a human cell line transformed by DNA from human adenovirus type 5. J. Gen. Virol. **36:**59–72.
30. **Haffer, O., J. Garrigues, B. Travis, P. Moran, J. Zarling, and S. L. Hu.** 1990. Human immunodeficiency virus-like, nonreplicating, *gag-env* particles assemble in a recombinant vaccinia virus expression system. J. Virol. **64:**2653–2659.
31. **Harrison, G. P., and A. M. Lever.** 1992. The human immunodeficiency virus type 1 packaging signal and major splice donor region have a conserved stable secondary structure. J. Virol. **66:**4144–4153.
32. **Hayashi, T., T. Shioda, Y. Iwakura, and H. Shibuta.** 1992. RNA packaging signals of human immunodeficiency virus type 1. Virology **188:**590–599.
33. **Jentoft, J. E., L. M. Smith, X. Fu, M. Johnson, and J. Leis.** 1988. Conserved cysteine and histidine residues of the avian myeloblastosis virus nucleocapsid protein are essential for viral replication but are not "zinc-binding fingers." Proc. Natl. Acad. Sci. USA **85:**7094–7098.
34. **Jowett, J. M. B., D. J. Hockley, M. V. Nermut, and I. M. Jones.** 1992. Distinct signals in human immunodeficiency virus type 1 Pr55 necessary for RNA binding and particle formation. J. Gen. Virol. **73:**3079–3086.
35. **Kaplan, A. H., J. A. Zack, M. Knigge, D. A. Paul, D. J. Kempf, D. W. Norbeck, and R. Swanstrom.** 1993. Partial inhibition of the human immunodeficiency virus type 1 protease results in aberrant virus assembly and the formation of noninfectious particles. J. Virol. **67:**4050–4055.
36. **Karacostas, V., K. Nagashima, M. A. Gonda, and B. Moss.** 1989. Human immunodeficiency virus-like particles produced by a vaccinia virus expression vector. Proc. Natl. Acad. Sci. USA **86:**8964–8967.
37. **Karpel, R. L., L. E. Henderson, and S. Oroszlan.** 1987. Interactions of retroviral structural proteins with single-stranded nucleic acids. J. Biol. Chem. **262:**4961–4967.
38. **Katz, R. A., R. W. Terry, and A. M. Skalka.** 1986. A conserved *cis*-acting sequence in the 5′ leader of avian sarcoma virus RNA is required for packaging. J. Virol. **59:**163–167.
39. **Kaye, J. F., and A. M. L. Lever.** 1996. *trans*-Acting proteins involved in RNA encapsidation and viral assembly in human immunodeficiency virus type 1. J. Virol. **70:**880–886.
40. **Khan, R., and D. P. Giedroc.** 1994. Nucleic acid binding properties of recombinant Zn^{2+} HIV-1 nucleocapsid protein are modulated by COOH-terminal processing. J. Biol. Chem. **269:**22538–22546.
41. **Khan, R., and P. Giedroc.** 1992. Recombinant human immunodeficiency virus type 1 nucleocapsid (NCp7) protein unwinds tRNA. J. Biol. Chem. **267:**6689–6695.
42. **Kim, H. J., K. Lee, and J. J. O'Rear.** 1994. A short sequence upstream of the 5′ major splice site is important for encapsidation of HIV-1 genomic RNA. Virology **198:**336–340.
43. **Kimpton, J., and M. Emerman.** 1992. Detection of replication-competent and pseudotyped human immunodeficiency virus with a sensitive cell line on the basis of activation of an integrated β-galactosidase gene. J. Virol. **66:**2232–2239.
44. **Knight, J. B., Z. H. Si, and C. M. Stoltzfus.** 1994. A base-paired structure in the avian sarcoma virus 5′ leader is required for efficient encapsidation of RNA. J. Virol. **68:**4493–4502.
45. **Kohl, N. E., E. A. Emini, W. A. Schleif, L. J. Davis, J. C. Heimbach, R. A. F. Dixon, E. M. Scolnick, and I. S. Sigal.** 1988. Active human immunodeficiency virus protease is required for viral infectivity. Proc. Natl. Acad. Sci. USA **85:**4686–4690.
46. **Konings, D. A. M., M. A. Nash, J. V. Maizel, and R. B. Arlinghaus.** 1992. Novel GACG-hairpin pair motif in the 5′ untranslated region of type C retroviruses related to murine leukemia virus. J. Virol. **66:**632–640.

47. **Laemmli, U. K.** 1970. Cleavage of structural proteins during the assembly of the head of bacteriophage T4. Nature (London) **227:**680–685.
48. **Lapadat-Tapolsky, M., C. Pernelle, C. Borie, and J. L. Darlix.** 1995. Analysis of the nucleic acid annealing activities of nucleocapsid protein from HIV-1. Nucleic Acids Res. **23:**2434–2441.
49. **Leis, J., and J. Jentoft.** 1983. Characteristics and regulation of interaction of avian retrovirus pp12 protein with viral RNA. J. Virol. **48:**361–369.
50. **Lever, A., H. Gottlinger, W. Haseltine, and J. Sodroski.** 1989. Identification of a sequence required for efficient packaging of human immunodeficiency virus type 1 RNA into virions. J. Virol. **63:**4085–4087.
51. **Linial, M. L., and A. D. Miller.** 1990. Retroviral RNA packaging: sequence requirements and implications. Curr. Top. Microbiol. Immunol. **157:**125–152.
52. **Long, C. W., L. E. Henderson, and S. Oroszlan.** 1980. Isolation and characterization of low-molecular-weight DNA-binding proteins from retroviruses. Virology **104:**491–496.
53. **Luban, J., and S. P. Goff.** 1991. Binding of human immunodeficiency virus type 1 (HIV-1) RNA to recombinant HIV-1 Gag polyprotein. J. Virol. **65:**3203–3212.
54. **Luban, J., and S. P. Goff.** 1994. Mutational analysis of *cis*-acting packaging signals in human immunodeficiency virus type 1 RNA. J. Virol. **68:**3784–3793.
55. **Maniatis, T., E. F. Fritsch, and J. Sambrook.** 1982. Molecular cloning: a laboratory manual. Cold Spring Harbor Laboratory, Cold Spring Harbor, N.Y.
56. **McBride, M. S., and A. T. Panganiban.** 1996. The human immunodeficiency virus type 1 encapsidation site is a multipartite RNA element composed of functional hairpin structures. J. Virol. **70:**2963–2973.
57. **McBride, M. S., and A. T. Panganiban.** 1997. Position dependence of functional hairpins important for human immunodeficiency virus type 1 RNA encapsidation in vivo. J. Virol. **71:**2050–2058.
58. **McBride, M. S., M. D. Schwartz, and A. T. Panganiban.** 1997. Efficient encapsidation of human immunodeficiency virus type 1 vectors and further characterization of *cis* elements required for encapsidation. J. Virol. **71:** 4544–4554.
59. **Meric, C., J. Darlix, and P. Spahr.** 1984. It is Rous sarcoma virus protein p12 and not p19 that binds tightly to Rous sarcoma virus RNA. J. Mol. Biol. **173:**531–538.
60. **Mervis, R. J., N. Ahmad, E. P. Lillehog, M. G. Raum, F. H. R. Salazar, H. G. Chan, and S. Venkatesan.** 1988. The *gag* gene products of human immunodeficiency virus type 1: alignment within the *gag* open reading frame, identification of posttranslational modifications, and evidence for alternative *gag* precursors. J. Virol. **62:**3993–4002.
61. **Oertle, S., and P.-F. Spahr.** 1990. Role of the *gag* polyprotein precursor in packaging and maturation of Rous sarcoma virus genomic RNA. J. Virol. **64:** 5757–5763.
62. **Ottmann, M., C. Cabus, and J. L. Darlix.** 1995. The central globular domain of the nucleocapsid protein of human immunodeficiency virus type 1 is critical for virion structure and infectivity. J. Virol. **69:**1778–1784.
63. **Page, K. A., N. R. Landau, and D. R. Littman.** 1990. Construction and use of a human immunodeficiency virus vector for analysis of virus infectivity. J. Virol. **64:**5270–5276.
64. **Parolin, C., T. Dorfman, G. Palu, H. Gottlinger, and J. Sodroski.** 1994. Analysis in human immunodeficiency virus type 1 vectors of *cis*-acting sequences that affect gene transfer into human lymphocytes. J. Virol. **68:**3888–3895.
65. **Peng, C., B. K. Ho, T. W. Chang, and N. T. Chang.** 1989. Role of human immunodeficiency virus type 1-specific protease in core protein maturation and viral infectivity. J. Virol. **63:**2550–2556.
66. **Poon, D. T. K., J. Wu, and A. Aldovini.** 1996. Charged amino acid residues of human immunodeficiency virus type 1 nucleocapsid p7 protein involved in RNA packaging and infectivity. J. Virol. **70:**6607–6616.
67. **Prats, A. C., L. Sarih, C. Gabus, S. Litvak, G. Keith, and J. L. Darlix.** 1988. Small finger protein of avian and murine retroviruses has nucleic acid annealing activity and positions the replication primer tRNA onto genomic RNA. EMBO J. **7:**1777–1783.
68. **Richardson, J. H., L. A. Child, and A. M. L. Lever.** 1993. Packaging of human immunodeficiency virus type 1 RNA requires *cis*-acting sequences outside of the 5′ leader region. J. Virol. **67:**3997–4005.
69. **Rizvi, T. A., and A. T. Panganiban.** 1993. Simian immunodeficiency virus RNA is efficiently encapsidated by human immunodeficiency virus type 1 particles. J. Virol. **67:**2681–2688.
70. **Sakalian, M., J. W. Wills, and V. M. Vogt.** 1994. Efficiency and selectivity of RNA packaging by Rous sarcoma virus Gag deletion mutants. J. Virol. **68:**5969–5981.
71. **Schmalzbauer, E., B. Strack, J. Dannull, S. Guehmann, and K. Moelling.** 1996. Mutations of basic amino acids of NCp7 of human immunodeficiency virus type 1 affect RNA binding in vitro. J. Virol. **70:**771–777.
72. **Shank, P. R., and M. Linial.** 1980. Avian oncovirus mutant (SE21Q1b) deficient in genomic RNA: characterization of a deletion in the provirus. J. Virol. **36:**450–456.
73. **Sheng, N., and S. Erickson-Viitanen.** 1994. Cleavage of p15 protein in vitro by human immunodeficiency virus type 1 protease is RNA dependent. J. Virol. **68:**6207–6214.
74. **Spearman, P., J.-J. Wang, N. Vander Heyden, and L. Ratner.** 1994. Identification of human immunodeficiency virus type 1 Gag protein domains essential to membrane binding and particle assembly. J. Virol. **68:**3232–3242.
75. **Tsuchihashi, Z., and P. O. Brown.** 1994. DNA annealing promoted by the human immunodeficiency virus type 1 nucleocapsid protein. J. Virol. **68:** 5863–5870.
76. **Wang, C.-T., and E. Barklis.** 1993. Assembly, processing, and infectivity of human immunodeficiency virus type 1 Gag mutants. J. Virol. **67:**4264–4273.
77. **Wills, J., and R. Craven.** 1991. Form, function, and use of retroviral gag proteins. AIDS **5:**639–654.
78. **Yang, S., and H. M. Temin.** 1994. A double hairpin structure is necessary for the efficient encapsidation of spleen necrosis virus retroviral RNA. EMBO J. **13:**713–726.
79. **Zhang, Y., and E. Barklis.** 1995. Nucleocapsid protein effects on the specificity of retrovirus RNA encapsidation. J. Virol. **69:**5716–5722.
80. **Zhou, W., L. J. Parent, J. W. Wills, and M. D. Resh.** 1994. Identification of a membrane-binding domain within the amino-terminal region of the human immunodeficiency virus type 1 Gag protein which interacts with acidic phospholipids. J. Virol. **68:**2556–2569.